symmetry

MDPI

Article

An Axisymmetric Problem of Suspension Filtering with Formation of Elastic–Plastic Cake Layer

Bakhtiyor Kh. Khuzhayorov [1], Usmonali Saydullaev [1], Gafurjan Ibragimov [2] and Nadihah Wahi [2,*]

[1] Department of Applied Mathematics, Samarkand State University, 15, University Str., Samarkand 140100, Uzbekistan; b.khuzhayorov@mail.ru (B.K.K.); saydullayev@samdu.uz (U.S.)
[2] Department of Mathematics and Statistics, and Institute for Mathematical Research, Faculty of Science, University Putra Malaysia, Seri Kembangan 43400, Malaysia; ibragimov@upm.edu.my
* Correspondence: nadihah@upm.edu.my

Abstract: The paper considers an axisymmetric problem of filtering suspensions with the formation of a cake on the filter surface. It is supposed that the cake has elastic–plastic properties. Using the mass conservation equation and Darcy's law, the suspension filtration equations at the elastic–plastic regime are derived, which characterize the partial irreversibility of the filtration characteristics when the system is unloaded after loading. An equation is also derived that describes the increase in the thickness of the cake. Problems of suspension filtering for the derived equations are posed and numerically solved. The role of partial irreversibility of deformation on the filtration characteristics is estimated. Distributions of compression pressure, the concentration of solid particles in the cake, relative permeability in the mode of primary and secondary loading of the system, as well as in the mode of unloading after the first loading are obtained. The growth dynamics of the cake thickness are also established. The parameters of plasticity in terms of particle concentration and permeability mainly affect the corresponding indicators, i.e., on the particle concentration distribution and on the relative permeability of the cake. It is shown, that depending on the change in the model parameters characterizing the elastic–plastic properties of the cake, the filtration characteristics change significantly. This indicates a significant effect of the elastic–plastic deformation of the cake on the suspension filtration characteristics.

Keywords: cake characteristics; cake filtration; concentration; elasto-plasticity; permeability; porosity; compression pressure

Citation: Khuzhayorov, B.K.; Saydullaev, U.; Ibragimov, G.; Wahi, N. An Axisymmetric Problem of Suspension Filtering with Formation of Elastic–Plastic Cake Layer. *Symmetry* **2022**, *14*, 1202. https://doi.org/10.3390/sym14061202

Academic Editors: Raffaele Barretta and Sergei Alexandrov

Received: 29 March 2022
Accepted: 17 May 2022
Published: 10 June 2022

1. Introduction

The filtration process is widely used in many fields of human activity. When filtering suspension clarification, filters with various design and technical characteristics are used [1–7]. In oil and gas, mining, chemical, and food industries, as well as environmental protection, ecology, etc., filtration is the basis of different technological processes. The clarification of various mixtures is also widely applied in biology and biotechnology [8–12].

In the process of suspension filtering through a porous filter, the solid phase (solid particles) is separated from the liquid phase and deposited on the outer surface of the filter. The latter is called the cake, which grows in thickness during the filtration process. The filtration and physico-mechanical characteristics of the cake determine the efficiency of cleaning the suspension from solid particles by filtration.

To analyze the filtration processes of various mixtures, in particular suspensions, one of the effective methods of analysis is mathematical modeling. Many works are devoted to mathematical modeling of the processes of filtering various mixtures. The study of [13] considered mathematical models of suspension filtration with the formation of a cake on various filter wall geometries. As an example of three-dimensional filtration, the growth of filtration sediment on a spherical partition was theoretically and experimentally studied in [14].

Baffles with a large radius of curvature for rotating drum vacuum filters are flat filter surfaces. Since the radius of curvature of the filter partition in cartridge filters is relatively small, the thickness of the sediment formed on the outer filtering surface and the thickness of the partition are comparable to the radius of curvature. Therefore, the boundary of the suspension and sediment layer and the boundary of the sediment layer and cylindrical filter wall are significantly different. As a result, the flow of the liquid phase of the suspension through the cake layer and the filtering baffle becomes more complicated.

In cartridge filters, the radius of the curvature of the filter elements is comparable to the thickness of the formed sediment; therefore, the filtration patterns become much more complicated. The filter element has a cylindrical shape, through the inner or outer side surface through which the suspension is fed. To describe the filtration process with compressible sediment formed on the cylindrical elements of cartridge filters, the axisymmetric Stefan problem must be formulated [6].

Suspension particles either linger on the filter surface, forming a precipitate, which is called a cake, or penetrate the filter, eventually being deposited in the pores. Accordingly, a distinction is made between cake filtration and pore-blocking filtration, i.e., deep bed filtration [3,6]. A cake is usually formed when the average particle diameter of the suspension is comparable to or greater than the average pore diameters of the filter. However, in many real cases, suspensions are polydisperse with a wide statistical distribution of particles in diameter (size), which can be either large or small compared to the average pore size. In this case, the deposition of particles occurs both on the surface and inside the pore space of the filter, i.e., cake and deep bed filtration are observed at the same time. However, models corresponding to this process have not yet been created. One of the first approaches to the analysis of such a filtering process was shown in [15], where a new mathematical model for cake formation with deep bed filtration for two-particle-size injection was proposed.

Studies of suspension filtration with formation of a cake [16–19] led to the development of the traditional theory of cake filtration. Suspension filtration models are based on volume-averaged equations of continuity, conservation of momentum and properties of a suspension and filter. In general, models of suspension filtration through porous media at low flow rates or low-pressure decreases are represented by Darcy's law [20–29]. The concept of cake resistivity is given in the primary work of Ruth et al. [16]. The pressure in the solid phase p_s, which is called compressive pressure, increases from the suspension–cake layer boundary to the cake–layer–baffle boundary. The pressure in the liquid phase p_ℓ decreases from the suspension–cake–layer interface to the cake–layer–baffle interface [26].

The authors of [4] studied the effect of $p_s - p_\ell$ on cake formation. Three different dependences of $p_s - p_\ell$ were considered, for which the numerical solutions of the filtering equation were compared with experimental data.

The authors of [6] presented experiments on filtration with sedimentation and showed the relative deformation curves of some sediments obtained with an increase and subsequent decrease in external pressure. Studies show that with the decrease in external pressure, the partial swelling of precipitation occurs. This means that the deformation of the cake is not purely elastic. Therefore, there are also plastic deformations of the cake when the system is loaded, which means that the cake does not fully restore its physical and mechanical characteristics after the removal of external pressure. Moreover, to the best of our knowledge, [30,31] there is no theory yet describing this phenomenon. In other words, a theory of elastic–plastic deformation of the cake has not yet been created. Until now, the cake has mainly been considered as a medium, the deformation of which occurs in a purely elastic regime. Many studies where the cake layer is considered as an elastically deformable medium can be identified [32,33]. When loading the system by creating a pressure difference or creating a filtration rate, the cake is deformed and it consolidates, causing changes in the porosity, permeability, concentration of solid particles, etc. This should be considered in the mathematical modeling of the process. In [34,35], a model of filtration was proposed for filtering suspensions with the formation of a cake, in which the filtration law had relaxation properties. Based on the numerical implementation of

the model, the influence of relaxation properties on the filtration characteristics is shown. Relaxation reflects the non-equilibrium nature of the filtration law in the cake. Like the residual deformations of the cake after unloading, the relaxation of the filtration law is a violation of the usual filtration law. In this case, the classical theory of filtration with cake formation must be generalized.

In this paper, a mathematical model of the suspension filtration process is considered, where the resulting cake has elastic–plastic properties. A cylindrical filter cartridge vertically installed in the suspension was considered. On the outer surface of the cartridge, because of separation of the suspension, a cake was formed, and its thickness continuously increased during the filtration process. At first, we derived the equations for filtering a suspension through a radial filter formed by an elastic–plastic cake. To model the elastic–plastic properties of sediment, we used the general principles of elastic–plastic filtration developed in [30,31,36–39]. First, the derivation of the filtration equations with increasing pressure was given, i.e., in the cake loading mode, and then in the unloading mode, i.e., when pressure is released. Separately, the suspension filtration equations were derived under repeated loading of the system, i.e., when the filtering mode was resumed. The model was implemented numerically, and the influence of the elasto-plasticity of the cake on the filtration characteristics was established.

2. Derivation of Equations

Let us consider the process of filtering a suspension through a cylindrical filter with the formation of the cake (Figure 1). In the process of filtration in the time interval $0 \le t \le T_1$, a cake is formed on the filter surface, in which the pressure increases in the range $0 \le p_s \le p_s^{(1)}$ i.e., a sludge loading process occurs in which the permeability and solids concentration of solid particles of the cake is changed such that the permeability decreases from k^0 to some values and the particles concentration increases from ε_s^0 to some values.

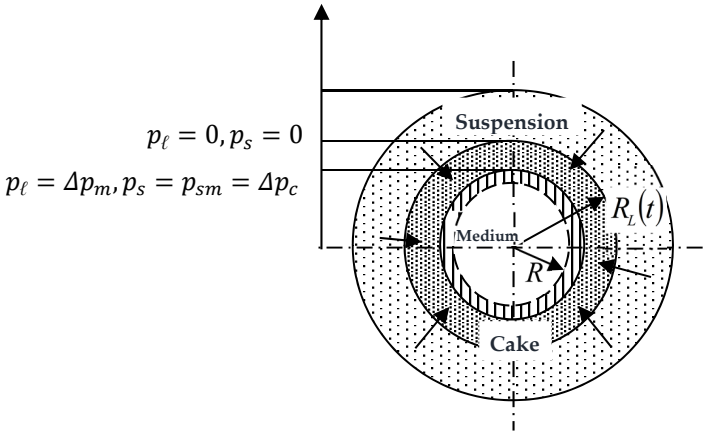

Figure 1. A schematic of filtering suspensions through a cylindrical filter.

We suppose that, as in [4], the permeability and concentration of solid particles changed according to power laws:

$$\uparrow k = k^0 \left(1 + \frac{p_s}{p_A}\right)^{-\delta} \tag{1}$$

$$\uparrow \varepsilon_s = \varepsilon_s^0 \left(1 + \frac{p_s}{p_A}\right)^{\beta} \tag{2}$$

where the sign $\uparrow$ means the pressure increase mode; ε_s^0, k^0 are values of ε_s, k at $p_s = 0$, respectively; p_A is characteristic pressure; and β, δ are exponents (constant values).

At some point in time $t = T_1$, the pressure is removed, and the filtration process stops, i.e., unloading begins the removal of the load. When the pressure p_s drops to zero, the permeability due to the restoration of the sediment structure (swelling) increases to a value $k^{(1)}$, which is less than the initial value k^0, and the concentration of solid particles ε_ε is restored to $\varepsilon_s^{(1)}$, which is higher than ε_s^0, i.e., the cake is not restored to its original state. If $k^{(1)} = k^0$ and $\varepsilon_s^{(1)} = \varepsilon_s^0$, there is a complete elastic recovery of the cake.

In the process of unloading, the change in the permeability and concentration of solid particles occurs with the same power laws (1) and (2), but with different coefficients and exponents:

$$\downarrow k = k^0 \left(1 + \frac{p_s^{(1)}}{p_A}\right)^{\delta_1 - \delta} \left(1 + \frac{p_s}{p_A}\right)^{-\delta_1} \tag{3}$$

$$\downarrow \varepsilon_s = \varepsilon_s^0 \left(1 + \frac{p_s^{(1)}}{p_A}\right)^{\beta - \beta_1} \left(1 + \frac{p_s}{p_A}\right)^{\beta_1} \tag{4}$$

where the sign $\downarrow$ means the pressure reduction mode, and $p_s^{(1)}$ is the pressure of the beginning of the unloading process; the exponents β_1, δ_1 of the dependence also have power law characteristics:

$$\delta_1 = \delta \left(1 + \frac{p_s^{(1)}}{p_A}\right)^{-\gamma_k} \tag{5}$$

$$\beta_1 = \beta \left(1 + \frac{p_s^{(1)}}{p_A}\right)^{-\gamma_\varepsilon} \tag{6}$$

where γ_ε and γ_k are exponents. If $\gamma_\varepsilon = 0$, $\gamma_k = 0$, we have a purely elastic regime.

If we repeat the filtration process, then in the range $0 \le p_s \le p_s^{(1)}$, the permeability decreases, and the concentration of solid particles will increase with the same pattern as under load, i.e., in accordance with laws (3) and (4) up to $p_s \le p_s^{(1)}$:

$$\uparrow\uparrow \varepsilon_s = \varepsilon_s^0 \left(1 + \frac{p_s^{(1)}}{p_A}\right)^{\beta - \beta_1} \left(1 + \frac{p_s}{p_A}\right)^{\beta_1}, \; p_s \le p_s^{(1)} \tag{7}$$

$$\uparrow\uparrow k = k^0 \left(1 + \frac{p_s^{(1)}}{p_A}\right)^{\delta_1 - \delta} \left(1 + \frac{p_s}{p_A}\right)^{-\delta_1}, \; p_s \le p_s^{(1)} \tag{8}$$

where $\uparrow\uparrow$ means the reloading mode.

When the pressure p_s reaches $p_s^{(1)}$, the filtration mode will change to the previous first loading mode.

In the range $p_s^{(1)} \le p_s \le p_s^{(2)}$, the permeability decreases according to the same dependence as before unloading. When $p_s = p_s^{(2)}$ again the filtration process stops and unloading begins. The permeability is restored to a value $k^{(2)}$ that is less than the value of $k^{(1)}$. The change of ε_s occurs in the same way as for k, with the only difference that the restored values ε_s will be higher than ε_s^0.

With subsequent loading, the process is similarly repeated. One can notice the fact that the greater the pressure p_s from which unloading begins, the more the recovered values $\varepsilon_s^{(1)}$, $k^{(1)}$ and $\varepsilon_s^{(2)}$, differ from the initial ones $\varepsilon_s^{(0)}$, $k^{(0)}$.

We will use the noted characteristic phenomena when compiling a filtration model with the formation of an elastic–plastic cake.

In the pressure increase mode, the filtration equation has the form:

$$\uparrow \frac{\partial \varepsilon_s}{\partial t} = -\frac{1}{r}\frac{\partial}{\partial r}\left(\varepsilon_s \cdot r \frac{k}{\mu}\frac{\partial p_\ell}{\partial r}\right) - \frac{q_{\ell m}}{2\pi} \cdot \frac{1}{r}\frac{\partial \varepsilon_s}{\partial r} \tag{9}$$

where $q_{\ell m} = \left[-2\pi r \frac{k}{\mu}\frac{\partial p_\ell}{\partial r}\right]_{r=R}$ is filtrate flow rate at the filter outlet.

Let us give an equation for the moving radius $R_L(t)$, which expresses the thickness of the cylindrical cake, i.e., border radius between suspension and cake layer:

$$\frac{dR_L}{dt} = \frac{\varepsilon_s^0}{\varepsilon_s^0 - \varepsilon_{s_0}}\left[\frac{k}{\mu}\frac{\partial p_\ell}{\partial r}\right]_{r=R_{L^-}} + \frac{1}{2\pi R_{L^-}} q_{\ell m} \tag{10}$$

At the surface $r = R_{L^-}$, the compressive stress particles are equal to zero, so $\varepsilon_s|_{R_{L^-}}$ can be taken equal to ε_s^0, the solid content at zero stress. On the other hand, $\varepsilon_s|_{R_{L^+}}$ is equal to the concentration of solid particles in the suspension ε_{s_0}.

If the process starts in a new filter without preliminary pumping of liquid, then we can accept the initial condition:

$$R_L(0) = R \tag{11}$$

If the filtration process begins with a sudden application of pressure or a flow velocity, the initial conditions for p_ℓ and p_s can be considered as zero, i.e.:

$$p_\ell(0,r) = 0,\ p_s(0,r) = 0 \tag{12}$$

The boundary conditions of the problem are taken in the form:

$$p_\ell = p_0,\ p_s = 0,\ \varepsilon_s = \varepsilon_s^0 \text{ when } r = R_L(t), \tag{13a}$$

$$-2\pi r \frac{k}{\mu}\frac{\partial p_\ell}{\partial r} = \frac{-p_\ell}{R_m \mu} \text{ when } r = R \tag{13b}$$

In the unloading mode, zero is taken as the time reference. Using (3) and (4) we derive the following filtering equation:

$$\downarrow \frac{\partial \varepsilon_s}{\partial t} = \frac{k^0 \varepsilon_s^0}{\mu}\frac{1}{r}\frac{\partial}{\partial r}\left(\left(1 + \frac{p_s^{(1)}}{p_A}\right)^{\beta-\beta_1+\delta-\delta_1}\left(1 + \frac{p_s}{p_A}\right)^{\beta_1-\delta_1} r\frac{\partial p_s}{\partial r}\right) - \frac{q_{\ell m}}{2\pi}\cdot\frac{1}{r}\frac{\partial \varepsilon_s}{\partial r} \tag{14}$$

The initial and boundary conditions can be specified as follows:

$$\downarrow p_s(0,x) = \uparrow p_s(T_1,x) = p_s^{(1)} \tag{15}$$

$$\downarrow p_s(t, R_L(t)) = 0,\ \downarrow p_s(t,0) = 0 \tag{16}$$

We assume that in the unloading mode, the cake does not grow, so that $R_L(t)$ remains unchanged, with the value $R_L(T_1)$.

In the reloading mode, a filtering equation is derived that coincides in form with (14) and (9):

$$\begin{aligned} \uparrow\uparrow \frac{\partial \varepsilon_s}{\partial t} &= \frac{k^0 \varepsilon_s^0}{\mu}\frac{1}{r}\frac{\partial}{\partial r}\left(\left(1 + \frac{p_s^{(1)}}{p_A}\right)^{\beta-\beta_1+\delta-\delta_1}\left(1 + \frac{p_s}{p_A}\right)^{\beta_1-\delta_1} r\frac{\partial p_s}{\partial r}\right) - \frac{q_{\ell m}}{2\pi}\cdot\frac{1}{r}\frac{\partial \varepsilon_s}{\partial r},\ p_s \le p_s^{(1)} \\ \uparrow\uparrow \frac{\partial \varepsilon_s}{\partial t} &= -\frac{1}{r}\frac{\partial}{\partial r}\left(\varepsilon_s \cdot r\frac{k}{\mu}\frac{\partial p_\ell}{\partial r}\right) - \frac{q_{\ell m}}{2\pi}\cdot\frac{1}{r}\frac{\partial \varepsilon_s}{\partial r},\ p_s \ge p_s^{(1)} \end{aligned} \tag{17}$$

Let the unloading process be completed in time T_2. During this time, zero pressure p_s is established in the entire thickness of the cake. The re-loading of the system can be started with a given pressure on $r = R$: $p_s = p_0^{(1)}$, where $p_0^{(1)}$ is the given pressure, it may

differ from the given pressure p_0 during the first loading. Then, the initial and boundary conditions for pressure have the following form (time again starts from zero):

$$\uparrow\uparrow p_s(0,r) = 0 \tag{18}$$

$$\uparrow\uparrow p_s = 0,\ \varepsilon_s = \varepsilon_s^0 \text{ when } r = R_L(t), \tag{19}$$

$$-\uparrow\uparrow 2\pi r \frac{k}{\mu}\frac{\partial p_\ell}{\partial r} = \frac{-p_\ell}{R_m\mu} \text{ when } r = R. \tag{20}$$

3. Numerical Solutions

First, consider the loading regime. To solve the Equations (9)–(20) we use the finite differences method [40]. We introduce a uniform grid by t with the step τ $\bar{\omega}_\tau = \{t|t = t_j = j\tau, j = 0,1,\ldots,N, \tau N = T\}$, and a non-uniform grid by a coordinate r $\bar{\omega}_h = \{r|r = r_i = r_{i-1} + h_i,\ i = 1,2,\ldots,N,\ r_N = R_{L-}\}$ with the variable steps: $h_i > 0$ (Figure 2). We are to choose the step h_i from the segment $[r_i, r_{i+1}]$, so that the mobile boundary moves exactly one step along the time grid. This approach is known as the method of catching the front in a grid node [34,35,41]. We denote by $p_{s,i}^{j+1}$ the grid function corresponding to p_s. We approximate Equation (9) by an implicit difference scheme that is nonlinear with respect to the function $p_{s,i}^{j+1}$:

$$\begin{aligned}\frac{p_{s,i}^{j+1} - p_{s,i}^{j}}{\tau} = \frac{a\left(p_{s,i}^{j}\right)}{r_i}\frac{2}{h_i + h_{i+1}}\Bigg\{ b\left(p_{s,i+1/2}^{j+1}\right) r_{i+1/2}\frac{p_{s,i+1}^{j+1} - p_{s,i}^{j+1}}{h_{i+1}} - \\ - b\left(p_{s,i-1/2}^{j+1}\right) r_{i-1/2}\frac{p_{s,i}^{j+1} - p_{s,i-1}^{j+1}}{h_i}\Bigg\} - (q_{\ell m})_0^{j+1}\frac{1}{2\pi r_i}\frac{p_{s,i}^{j+1} - p_{s,i-1}^{j+1}}{h_i},\end{aligned} \tag{21}$$

$$i = 1,\ldots,N-1,\ \ j = 0,1,\ldots,N-1$$

where $r_{i-1/2} = \frac{r_{i-1}+r_i}{2}$, $r_{i+1/2} = \frac{r_{i+1}+r_i}{2}$, $a\left(p_{s,i}^{j}\right) = \frac{p_A k^0}{\beta\mu}\left(1 + \frac{p_{s,i}^{j}}{p_A}\right)^{1-\beta}$, $c^0\left(p_{s,0}^{j+1}\right) = \frac{k^0}{\mu}\left(1 + \frac{p_{s,0}^{j+1}}{p_A}\right)^{-\delta}$, $b\left(p_{s,i+1/2}^{j+1}\right) = \frac{1}{2}\left[\left(1 + \frac{p_{s,i+1}^{j+1}}{p_A}\right)^{\beta-\delta} + \left(1 + \frac{p_{s,i}^{j+1}}{p_A}\right)^{\beta-\delta}\right]$, $(q_{\ell m})_0^{j+1} = -2\pi r_1 c^0\left(p_{s,0}^{j+1}\right)\left(\frac{p_{s,1}^{j+1} - p_{s,0}^{j+1}}{h_0}\right)$.

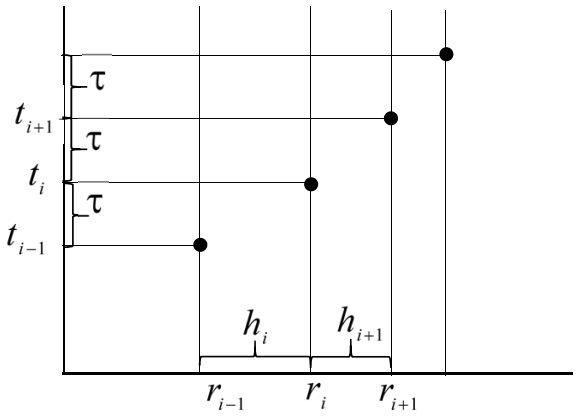

Figure 2. Introduction of new variables r, t for the problem on the continuous ingot.

Equation (10), when $\frac{dR_L}{dt} \approx \frac{h_{i+1}}{\tau}$ after the approximation, it can be written in the form:

$$\frac{h_{i+1}}{\tau} = -\left[c\left(p^j_{s,i-1/2}\right)\left(\frac{p^{j+1}_{s,i} - p^{j+1}_{s,i-1}}{h_{i+1}}\right)\right] - \frac{1}{2\pi r_i}(q_{\ell m})^{j+1}_0 \tag{22}$$

where $c\left(p^j_{s,i-1/2}\right) = \frac{\varepsilon^0_s}{\varepsilon^0_s - \varepsilon_{s_0}} \frac{k^0}{2\mu}\left[\left(1 + \frac{p^j_{s,i}}{p_A}\right)^{-\delta} + \left(1 + \frac{p^j_{s,i-1}}{p_A}\right)^{-\delta}\right]$.

The approximation of initial (12) and boundary conditions (13) gives:

$$p^j_{s,i} = 0,\ i = 0, 1, \ldots, N,\ j = 0$$

$$-2\pi r_1 \frac{k^0}{\mu}\left(1 + \frac{p^{j+1}_{s,0}}{p_A}\right)^{-\delta} \frac{p^j_{s,1} - p^j_{s,0}}{h_1} = \frac{p_0 - p^{j+1}_{s,0}}{\mu R_m},\ j = \overline{0, N} \tag{23}$$

$$p^{j+1}_{s,i} = 0,\ i = N+1, N+2, \ldots, j = 0, 1, \ldots$$

The obtained set of equations is nonlinear, so to solve it, we use the method of simple iteration and rewrite Equation (21) in the following form:

$$\frac{{}^{(\lambda+1)^{j+1}}_{p_{s,i}} - p^j_{s,i}}{\tau} = \frac{a\left(p^j_{s,i}\right)}{r_i}\frac{2}{h_i + h_{i+1}}\left\{b\left({}^{(\lambda)^{j+1}}_{p_{s,i+1/2}}\right) r_{i+1/2}\frac{{}^{(\lambda+1)^{j+1}}_{p_{s,i+1}} - {}^{(\lambda+1)^{j+1}}_{p_{s,i}}}{h_{i+1}} - b\left({}^{(\lambda)^{j+1}}_{p_{s,i-1/2}}\right) r_{i-1/2}\frac{{}^{(\lambda+1)^{j+1}}_{p_{s,i}} - {}^{(\lambda+1)^{j+1}}_{p_{s,i-1}}}{h_i}\right\} -$$
$$-\left({}^{(\lambda)}_{q_{\ell m}}\right)^{j+1}_0 \frac{1}{2\pi r_i}\frac{{}^{(\lambda+1)^{j+1}}_{p_{s,i}} - {}^{(\lambda+1)^{j+1}}_{p_{s,i-1}}}{h_i}, i = 1, \ldots, N-1,\ j = 0, 1, \ldots, N-1 \tag{24}$$

where $b\left({}^{(\lambda)^{j+1}}_{p_{s,i+1/2}}\right) = \frac{1}{2}\left[\left(1 + \frac{{}^{(\lambda)^{j+1}}_{p_{s,i+1}}}{p_A}\right)^{\beta-\delta} + \left(1 + \frac{{}^{(\lambda)^{j+1}}_{p_{s,i}}}{p_A}\right)^{\beta-\delta}\right]$, $\left({}^{(\lambda)}_{q_{\ell m}}\right)^{j+1}_0 = 2\pi r_1 c^0$ $\left({}^{(\lambda)^{j+1}}_{p_{s,0}}\right)\left(\frac{{}^{(\lambda)^{j+1}}_{p_{s,1}} - {}^{(\lambda)^{j+1}}_{p_{s,0}}}{h_0}\right)$, λ is the number of iterations.

The system of Equation (24) is now linear with respect to ${}^{(\lambda+1)^{j+1}}_{p_{s,i}}$, which allows us to use the Tomas's algorithm. As a condition to stop iteration procedure on this time layer, the following relationship can be used:

$$\max_i \left| {}^{(\lambda+1)^{j+1}}_{p_{s,i}} - {}^{(\lambda)^{j+1}}_{p_{s,i}} \right| \le \chi, \tag{25}$$

where χ is the given accuracy of calculations. When Equation (25) is satisfied, then ${}^{(\lambda)^{j+1}}_{p_{s,i}} = p^j_{s,i}$.

Equation (24) leads to the system of linear equations:

$${}^{(\lambda)}_{A_i}{}^{(\lambda+1)^{j+1}}_{p_{s,i+1}} - {}^{(\lambda)}_{B_i}{}^{(\lambda+1)^{j+1}}_{p_{s,i}} + {}^{(\lambda)}_{C_i}{}^{(\lambda+1)^{j+1}}_{p_{s,i-1}} = {}^{(\lambda)}_{F_i},\ i = \overline{1, N-1}, \tag{26}$$

where ${}^{(\lambda)}_{A_i} = \frac{b\left({}^{(\lambda)^{j+1}}_{p_{s,i+1/2}}\right)}{h_{i+1}} r_{i+1/2}$, ${}^{(\lambda)}_{C_i} = \frac{b\left({}^{(\lambda)^{j+1}}_{p_{s,i-1/2}}\right)}{h_i} r_{i-1/2} + \frac{h_{i+1}+h_i}{2a\left(p^j_{s,i}\right)}\frac{\left({}^{(\lambda)}_{q_{\ell m}}\right)^{j+1}_0}{2\pi h_{i+1}}$,

$$\overset{(\lambda)}{F_i} = -\frac{r_i}{2\tau}\cdot\frac{h_{i+1}+h_i}{a\left(p^j_{s,i}\right)}\overset{(\lambda)}{p}{}^{j}_{s,i},\ \overset{(\lambda)}{B_i} = \left[\frac{b\left(\overset{(\lambda)}{p}{}^{j+1}_{s,i+1/2}\right)}{h_{i+1}}r_{i+1/2}+\frac{b\left(\overset{(\lambda)}{p}{}^{j+1}_{s,i-1/2}\right)}{h_i}r_{i-1/2}\right]+\frac{h_{i+1}+h_i}{2a\left(p^j_{s,i}\right)}\frac{\left(\overset{(\lambda)}{q}{}_{\ell m}\right)^{j+1}_0}{2\pi h_{i+1}}$$

$$+\frac{r_i}{2\tau}\cdot\frac{h_{i+1}+h_i}{a\left(p^j_{s,i}\right)}.$$

Equation (10) is used to determine the step coordinate and it can be written in the form:

$$(h_{i+1})^2-\frac{\tau}{2\pi r_i}(q_{\ell m})^{j+1}_0 h_{i+1}-\tau c\left(p^j_{s,i-1/2}\right)\left(p^{j+1}_{s,i}-p^{j+1}_{s,i-1}\right)=0. \tag{27}$$

By solving this nonlinear equation for each time layer, we can determine h_{i+1}.

The system of Equation (26) is solved by the Tomas' algorithm:

$$\overset{(\lambda+1)}{p}{}^{j+1}_{s,i} = \xi_{i+1}\overset{(\lambda+1)}{p}{}^{j+1}_{s,i+1}+\eta_{i+1} \tag{28}$$

where $\xi_{i+1}=\frac{\overset{(\lambda)}{A_i}}{\overset{(\lambda)}{B_i}-\overset{(\lambda)}{C_i}\xi_i}$, $\eta_{i+1}=\frac{\overset{(\lambda)}{-F_i}+\overset{(\lambda)}{C_i}\eta_i}{\overset{(\lambda)}{B_i}-\overset{(\lambda)}{C_i}\xi_i}$.

The starting values of the coefficients ξ_1 and η_1 are determined from the boundary conditions, which have the form:

$$\xi_1=\frac{R_m c^{(2)}\left(p^j_{s,i}\right)}{R_m c^{(2)}\left(p^j_{s,i}\right)+h_0},\ \eta_1=\frac{p_c h_0}{R_0 c^{(2)}\left(p^j_{s,i}\right)+1}$$

where $c^{(2)}\left(p^j_{s,i}\right)=2\pi r_i k^0\left(1+\frac{p^j_{s,i}}{p_A}\right)^{-\delta}$.

Now $t=T_1$, and the unloading regime begins. We calculate the derivatives $\frac{\partial\varepsilon_s}{\partial t}$ and $\frac{\partial\varepsilon_s}{\partial r}$ in (7) and (8) and substitute them into (14) to obtain the following equation with respect to p_s:

$$\downarrow\ \frac{\partial p_s}{\partial t}=a\left(p^{(1)}_s,p_s\right)\cdot\frac{1}{r}\frac{\partial}{\partial r}\left[b\left(p^{(1)}_s,p_s\right)\cdot r\frac{\partial p_s}{\partial r}\right]-w(p_s)\frac{q_{\ell m}}{2\pi r}\left[w_1\left(p^{(1)}_s\right)-w_2\left(p^{(1)}_s,p_s\right)\right]\frac{\partial p^{(1)}_s}{\partial r}-\frac{q_{\ell m}}{2\pi r}\frac{\partial p_s}{\partial x}, \tag{29}$$

where $a\left(p^{(1)}_s,p_s\right)=\frac{k^0 p_A}{\mu\beta_1}\left(1+\frac{p^{(1)}_s}{p_A}\right)^{\beta_1-\beta}\left(1+\frac{p_s}{p_A}\right)^{1-\beta_1}$, $b\left(p^{(1)}_s,p_s\right)=\left(1+\frac{p^{(1)}_s}{p_A}\right)^{\beta-\beta_1+\delta_1-\delta}\left(1+\frac{p_s}{p_A}\right)^{\beta_1-\delta_1}$,

$w(p_s)=\frac{1}{\beta_1}\left(1+\frac{p_s}{p_A}\right)$, $w_1\left(p^{(1)}_s\right)=\gamma_\varepsilon\beta_1\left(1+\frac{p^{(1)}_s}{p_A}\right)^{-1}ln\left(1+\frac{p^{(1)}_s}{p_A}\right)+(\beta-\beta_1)\left(1+\frac{p^{(1)}_s}{p_A}\right)^{-1}$,

$w_2\left(p^{(1)}_s,p_s\right)=\beta_1\gamma_\varepsilon\left(1+\frac{p^{(1)}_s}{p_A}\right)^{-1}ln\left(1+\frac{p_s}{p_A}\right)$.

To solve Equation (29) with Equations (15) and (16), we use the finite differences method.

We approximate Equation (29) in the form:

$$\begin{aligned}\frac{(p_s)^{j+1}_i-(p_s)^j_i}{\tau} &= a\left(p^{(1)}_s,p_s\right)^j_i\frac{1}{r_i}\frac{2}{h_{i+1}+h_i}\left[b\left(p^{(1)}_s,p_s\right)^{j+1}_{i+1/2}r_{i+\frac{1}{2}}\frac{(p_s)^{j+1}_{i+1}-(p_s)^{j+1}_i}{h_{i+1}}-\right.\\ &\left.-b\left(p^{(1)}_s,p_s\right)^{j+1}_{i-1/2}r_{i-\frac{1}{2}}\frac{(p_s)^{j+1}_i-(p_s)^{j+1}_{i-1}}{h_i}\right]-w(p_s)^j_i\frac{(q_{\ell m})^{j+1}_0}{2\pi r_i}\times\\ &\times\left[w_1\left(p^{(1)}_s\right)^j_i-w_2\left(p^{(1)}_s,p_s\right)^j_i\right]\frac{\left(p^{(1)}_s\right)_i-\left(p^{(1)}_s\right)_{i-1}}{h_i}-\frac{(q_{\ell m})^{j+1}_0}{2\pi r_i}\frac{(p_s)^{j+1}_i-(p_s)^{j+1}_{i-1}}{h_i},\\ & i=1,2,\ldots,N-1,\end{aligned} \tag{30}$$

where $r_{i-1/2}=\frac{r_{i-1}+r_i}{2}$, $r_{i+1/2}=\frac{r_{i+1}+r_i}{2}$, $a\left(p_s^{(1)},p_s\right)_i^j=\frac{k^0 p_A}{\mu\beta_1}\left(1+\frac{\left(p_s^{(1)}\right)_i}{p_A}\right)^{(\beta_1)_i^i-\beta}\left(1+\frac{(p_s)_i^j}{p_A}\right)^{1-(\beta_1)_i^j}$,

$b\left(p_s^{(1)},p_s\right)_{i+1/2}^{j+1}=\frac{1}{2}\left[\left(1+\frac{\left(p_s^{(1)}\right)_{i+1}}{p_A}\right)^{\beta-(\beta_1)_{i+1}+(\delta_1)_{i+1}-\delta}\left(1+\frac{(p_s)_{i+1}^{j+1}}{p_A}\right)^{(\beta_1)_{i+1}-(\delta_1)_{i+1}}+\right.$

$\left.+\left(1+\frac{\left(p_s^{(1)}\right)_i}{p_A}\right)^{\beta-(\beta_1)_i+(\delta_1)_i-\delta}\left(1+\frac{(p_s)_i^{j+1}}{p_A}\right)^{(\beta_1)_i-(\delta_1)_i}\right]$, $w(p_s)_i^j=\frac{1}{\beta_1}\left(1+\frac{(p_s)_i^j}{p_A}\right)$,

$w_1\left(p_s^{(1)}\right)_i^j=\gamma_\varepsilon(\beta_1)_i^j\left(1+\frac{\left(p_s^{(1)}\right)_i}{p_A}\right)^{-1}ln\left(1+\frac{\left(p_s^{(1)}\right)_i}{p_A}\right)+\left(\beta-(\beta_1)_i^j\right)\left(1+\frac{\left(p_s^{(1)}\right)_i}{p_A}\right)^{-1}$,

$w_2\left(p_s^{(1)},p_s\right)_i^j=(\beta_1)_i^j\gamma_\varepsilon\left(1+\frac{\left(p_s^{(1)}\right)_i}{p_A}\right)^{-1}ln\left(1+\frac{(p_s)_i^j}{p_A}\right)$, $(\delta_1)_i=\delta\left(1+\frac{\left(p_s^{(1)}\right)_i}{p_A}\right)^{-\gamma_k}$,

$(q_{\ell m})_0^{j+1}=\frac{k^0}{\mu}\left(1+\frac{\left(p_s^{(1)}\right)_i}{p_A}\right)^{(\delta_1)_i-\delta}\left(1+\frac{(p_s)_i^j}{p_A}\right)^{-(\delta_1)_i}\frac{(p_s)_1^{j+1}-(p_s)_0^{j+1}}{h_1}$, $(\beta_1)_i=\beta\left(1+\frac{\left(p_s^{(1)}\right)_i}{p_A}\right)^{-\gamma_\varepsilon}$.

The approximation of initial and boundary conditions gives:

$$\begin{gathered}(p_s)_i^j=p_s^{(1)},\ i=0,1,\ldots,N,\ j=0\\(p_s)_i^j=0,\ i=0,\ j=0,1,\ldots,N,(p_s)_i^j=0,\ i=N,\ j=0,1,\ldots N.\end{gathered}\tag{31}$$

The set of Equation (30) is nonlinear, so to solve it, we use the method of simple iteration. The iteration procedure takes the following form:

$$\frac{{}^{(\lambda+1)^{j+1}}_{p\ s,i}-(p_s)_i^j}{\tau}=a\left(p_s^{(1)},{}^{(\lambda)}_{p\ s}\right)_i^j\frac{1}{r_i}\frac{2}{h_{i+1}+h_i}\left[{}^{(\lambda)}_{b}\left(p_s^{(1)},p_s\right)_{i+\frac{1}{2}}^{j+1}\frac{1}{r_{i+\frac{1}{2}}}\frac{{}^{(\lambda+1)^{j+1}}_{p\ s,i+1}-{}^{(\lambda+1)^{j+1}}_{p\ s,i}}{h_{i+1}}-{}^{(\lambda)}_{b}\left(p_s^{(1)},{}^{(\lambda)}_{p\ s}\right)_{i-1/2}^{j+1}\times\right.$$

$$\left.\times\frac{1}{r_{i-\frac{1}{2}}}\frac{{}^{(\lambda+1)^{j+1}}_{p\ s,i}-{}^{(\lambda+1)^{j+1}}_{p\ s,i-1}}{h_i}\right]-w(p_s)_i^j\frac{\left({}^{(\lambda)}_{q\ \ell m}\right)_0^{j+1}}{2\pi r_i}\times\left[w_1\left(p_s^{(1)}\right)_i^j-w_2\left(p_s^{(1)},{}^{(\lambda)}_{p\ s}\right)_i^j\right]\frac{\left(p_s^{(1)}\right)_i-\left(p_s^{(1)}\right)_{i-1}}{h_i}\tag{32}$$

$$-\frac{\left({}^{(\lambda)}_{q\ \ell m}\right)_0^{j+1}}{2\pi r_i}\frac{{}^{(\lambda+1)^{j+1}}_{p\ s,i}-{}^{(\lambda+1)^{j+1}}_{p\ s,i-1}}{h_i},$$

where ${}^{(\lambda)}_{b}\left(p_s^{(1)},{}^{(\lambda)}_{p\ s}\right)_{i+1/2}^{j+1}=\frac{1}{2}\left[\left(1+\frac{\left(p_s^{(1)}\right)_{i+1}}{p_A}\right)^{\beta-(\beta_1)_{i+1}+(\delta_1)_{i+1}-\delta}\left(1+\frac{{}^{(\lambda)^{j+1}}_{p\ s,i+1}}{p_A}\right)^{(\beta_1)_{i+1}-(\delta_1)_{i+1}}+\right.$

$\left.+\left(1+\frac{\left(p_s^{(1)}\right)_i}{p_A}\right)^{\beta-(\beta_1)_i+(\delta_1)_i-\delta}\left(1+\frac{{}^{(\lambda)^{j+1}}_{p\ s,i}}{p_A}\right)^{(\beta_1)_i-(\delta_1)_i}\right]$,

$\left({}^{(\lambda)}_{q\ell m}\right)_0^{j+1}=\frac{k^0}{\mu}\left(1+\frac{\left(p_s^{(1)}\right)_i}{p_A}\right)^{(\delta_1)_i-\delta}\left(1+\frac{{}^{(\lambda)^j}_{p\ s,i}}{p_A}\right)^{-(\delta_1)_i}\frac{{}^{(\lambda)^{j+1}}_{p\ s,1}-{}^{(\lambda)^{j+1}}_{p\ s,0}}{h_1}$,

λ is the number of iterations.

The system of Equation (32) is linear with respect to ${}^{(\lambda+1)^{j+1}}_{p\ s,i}$, which allows Tomas's algorithm to be used.

Equation (32) lead to the system of linear equations:

$${}^{(\lambda)}_{A_i}{}^{(\lambda+1)^{j+1}}_{p\ s,i+1}-{}^{(\lambda)}_{B_i}{}^{(\lambda+1)^{j+1}}_{p\ s,i}+{}^{(\lambda)}_{C_i}{}^{(\lambda+1)^{j+1}}_{p\ s,i-1}={}^{(\lambda)}_{F_i},\ i=\overline{1,N-1}\tag{33}$$

where $\overset{(\lambda)}{A}_i = \frac{\overset{(\lambda)}{b}\left(p_s^{(1)}, \overset{(\lambda)}{p}_s\right)_{i+1/2}^{j+1}}{h_{i+1}} r_{i+\frac{1}{2}}$, $\overset{(\lambda)}{C}_i = \frac{\overset{(\lambda)}{b}\left(p_s^{(1)}, \overset{(\lambda)}{p}_s\right)_{i-1/2}^{j+1}}{h_i} r_{1-\frac{1}{2}} + \frac{h_{i+1}+h_i}{2h_i a\left(p_s^{(1)}, p_s\right)_i^j} \frac{\left(\overset{(\lambda)}{q}_{\ell m}\right)_0^{j+1}}{2\pi}$,

$\overset{(\lambda)}{B}_i = \frac{\overset{(\lambda)}{b}\left(p_s^{(1)}, \overset{(\lambda)}{p}_s\right)_{i+1/2}^{j+1}}{h_{i+1}} r_{1+\frac{1}{2}} + \frac{\overset{(\lambda)}{b}\left(p_s^{(1)}, \overset{(\lambda)}{p}_s\right)_{i-1/2}^{j+1}}{h_i} r_{1-\frac{1}{2}} + \frac{h_{i+1}+h_i}{2\tau a\left(p_s^{(1)}, p_s\right)_i^j} r_i + \frac{h_{i+1}+h_i}{2h_i a\left(p_s^{(1)}, p_s\right)_i^j} \frac{\left(\overset{(\lambda)}{q}_{\ell m}\right)_0^{j+1}}{2\pi}$,

$\overset{(\lambda)}{F}_i = -\left(\frac{h_{i+1}+h_i}{2\tau a\left(p_s^{(1)}, p_s\right)_i^j} r_i - \frac{h_{i+1}+h_i}{2a\left(p_s^{(1)}, p_s\right)_i^j} w(p_s)_i^j \frac{\left(\overset{(\lambda)}{q}_{\ell m}\right)_0^{j+1}}{2\pi} \left(w_1\left(p_s^{(1)}\right)_i^j - w_1\left(p_s^{(1)}, p_s\right)_i^j \right) \frac{\left(p_s^{(1)}\right)_i - \left(p_s^{(1)}\right)_{i-1}}{h_i} \right)$.

The fundamental relation for the Tomas' algorithm has the form:

$$\overset{(\lambda+1)}{p}{}_{s,i}^{j+1} = \xi_{i+1} \overset{(\lambda+1)}{p}{}_{s,i+1}^{j+1} + \eta_{i+1},\ i = \overline{0,\ N-1} \tag{34}$$

where $\xi_{i+1} = \frac{\overset{(\lambda)}{A}_i}{\overset{(\lambda)}{B}_i - \overset{(\lambda)}{C}_i \xi_i}$, $\eta_{i+1} = \frac{-\overset{(\lambda)}{F}_i + \overset{(\lambda)}{C}_i \eta_i}{\overset{(\lambda)}{B}_i - \overset{(\lambda)}{C}_i \xi_i}$.

The starting values of the coefficients ξ_1 and η_1 are determined from the boundary conditions, which have the form $\xi_1 = 0$, $\eta_1 = 0$.

Let us consider the solution of the filtering problem in the reloading mode. In this case, Equation (17) is solved with initial and boundary conditions (18)–(20).

Approximation of the initial and boundary conditions gives:

$$\begin{gathered} p_{s,i}^j = 0,\ i = 0, 1, \ldots, N,\ j = 0 \\ -k\left(p_{s,0}^j\right)_0^j \frac{p_{s,1}^j - p_{s,0}^j}{h_1} = \frac{p_0 - p_{s,0}^{j+1}}{R_m},\ j = \overline{0, N} \\ p_{s,i}^{j+1} = 0,\ i = N+1,\ N+2,\ \ldots,\ j = 0, 1, \ldots \end{gathered} \tag{35}$$

where $k\left(p_{s,0}^j\right)_0^j = 2\pi r_1 k^0 \left(1 + \frac{\left(p_s^{(1)}\right)_0}{p_A}\right)^{(\delta_1)_0 - \delta} \left(1 + \frac{(p_s)_0^j}{p_A}\right)^{-(\delta_1)_0}$.

The starting values of the coefficients ξ_1 and η_1 are determined from the boundary conditions (35), which have the form:

$$\xi_1 = \frac{R_m k\left(p_{s,0}^j\right)}{R_m k\left(p_{s,i}^j\right) + h_0},\ \eta_1 = \frac{p_c h_0}{R_0 k\left(p_{s,i}^j\right) + 1}$$

4. Results of Numerical Analysis

The numerical results of solving Equations (26) and (27) were obtained for the following parameter values: $p_A = 10^4$ Pa, $p_0 = 10^5$ Pa, $R_m = 10^{12}$ 1/m, $\mu = 10^{-3}\ Pa \cdot s$, $k^0 = 5 \cdot 10^{-13}$ m^2, $\varepsilon_s^0 = 0.20$, $\varepsilon_{s_0} = 0.0076$, $\beta = 0.13$, $\delta = 0.57$.

Some of the results are shown in Figure 3. As can be seen from the presented results, as the filtration process continues, the compression pressure decreases from the filter surface to the border of the cake and suspension (Figure 3a). The value ε_s monotonically decreases from the filter surface to the common border of the cake and suspension (Figure 3b). The relative permeability in the cake is shown in Figure 3c. As can be seen from the figure, as the thickness of the cake increases, the permeability decreases from the initial value k^0. As time increases along the thickness of the cake in the distribution of p_s and ε_s an increase in values is noted, and there is a decrease in k/k_0. This is due to the consolidation (compaction) of the cake with increasing time. The range of change in the graphs by r has a finite value, limited by the thickness of the cake. The dynamics of the cake layer thickness are shown below.

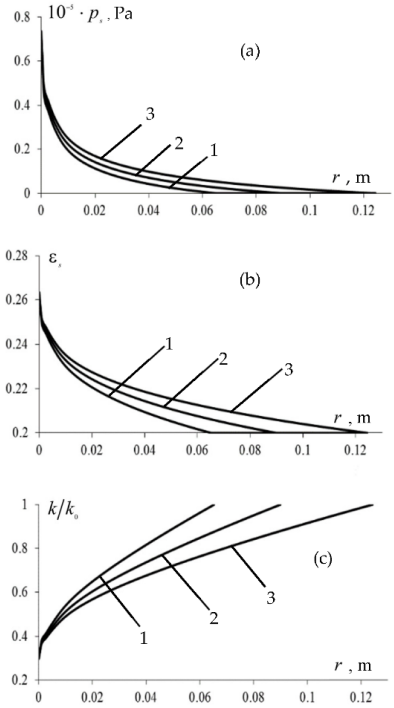

Figure 3. Distributions of p_s (**a**), ε_s (**b**), k/k_0 (**c**) at pressure increasing regimes: $t = 225$ (1); 450 (2); 900 (3) s.

Some results of numerical calculations using (33) and (34) are shown in Figures 4–6. From the curves in the figures, with the beginning of the unloading process at the boundary of the sediment and the filter, the pressure vanishes due to the hydraulic resistance of the filter. Porosity (curves b in Figures 4–6) and permeability (curves c in Figures 4–6) are not restored to their original values at the sediment–filter boundary, i.e., residual effects are observed. This is due to the plastic properties of the sediment.

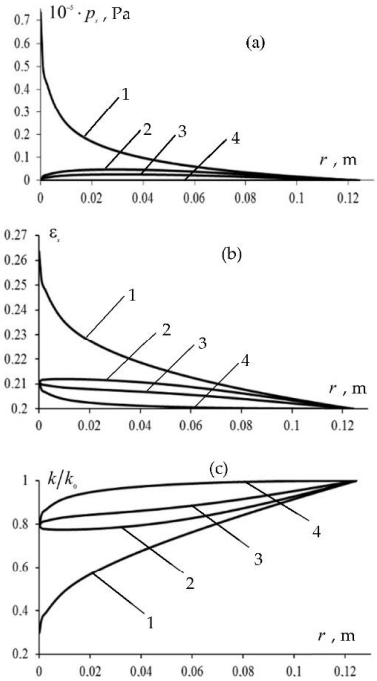

Figure 4. Distributions of p_s (**a**), ε_s (**b**), k/k_0 (**c**) at pressure decreasing regimes: $\gamma_\varepsilon = 0.1$, $\gamma_k = 0.1$, 1—($t = 0$ s), 2—($t = 25$ s), 3—($t = 50$ s), 4—($t = 300$ s).

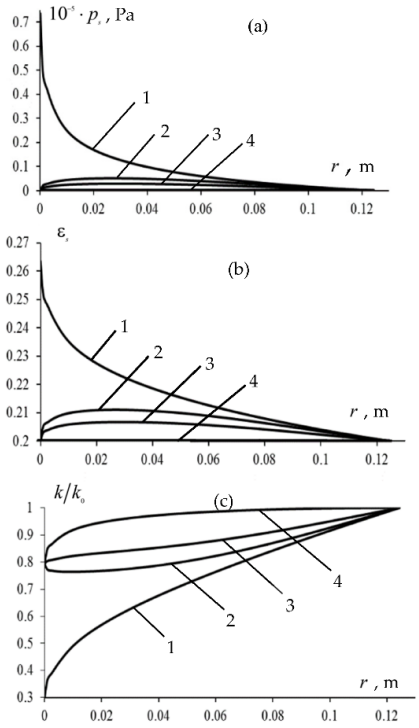

Figure 5. Distributions of p_s (**a**), ε_s (**b**), k/k_0 (**c**) at pressure decreasing regimes: $\gamma_\varepsilon = 0.001$, $\gamma_k = 0.1$, 1—($t = 0$ s), 2—($t = 25$ s), 3—($t = 50$ s), 4—($t = 300$ s).

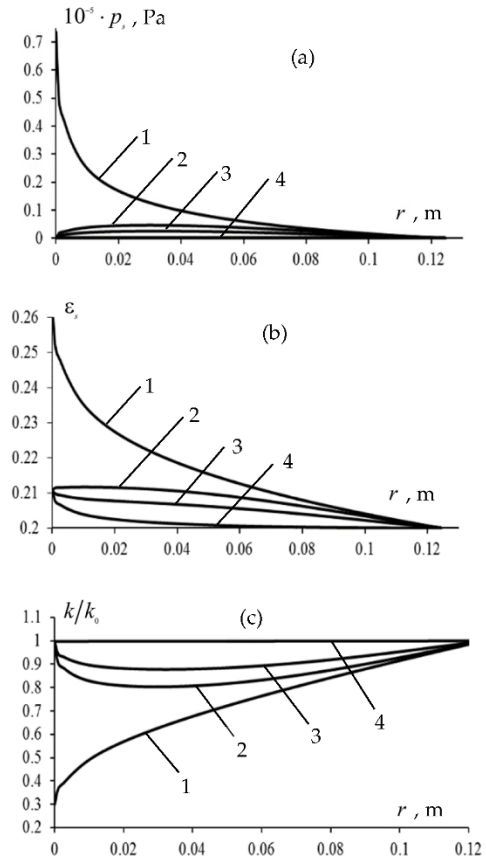

Figure 6. Distributions of p_s (**a**), ε_s (**b**), k/k_0 (**c**) at pressure decreasing regimes: $\gamma_\varepsilon = 0.1$, $\gamma_k = 0.001$, 1—($t = 0$ s), 2—($t = 25$ s), 3—($t = 50$ s), 4—($t = 300$ s).

As mentioned above, at $\gamma_\varepsilon = 0$, $\gamma_k = 0$ we have a purely elastic regime, when all the characteristics of the sediment layer after unloading are restored to their previous values. When these parameters are different from zero, plastic effects should appear. To show the influence of parameters γ_ε and γ_k on the filtration performance, calculations were carried out for a certain set of values of these parameters. Figures 4–6 are compiled for three pairs of values: γ_ε and γ_k.

The first case refers to the values of the parameters $\gamma_\varepsilon = 0.1$, $\gamma_k = 0.1$ (Figure 4). Over time, the compression pressure p_s gradually decreases to zero (Figure 4a). However, with increasing time, ε_s and k/k_0 do not fully reach their original values, which they had before the system was loaded. After removing the load at the border of the cake and the filter, ε_s decreases to ~0.21, and k/k_0 recovers to ~0.8. The results of decreasing the values of γ_ε and γ_k one by one up to 0.001 are shown in Figures 5 and 6, respectively. Reducing the value γ_ε from 0.1 to 0.001 mainly affects the distribution of ε_s. At the same time, the residual phenomena in the ε_s distribution weakens at the border of the filter, and the cake, ~0.202–0.203 is obtained, which is very close to the initial value of $\varepsilon_s^0 = 0.2$. The results when the γ_k value decreases from 0.1 to 0.001 at $\gamma_\varepsilon = 0.1$ are shown in Figure 6.

For this case, the main changes occur in the k/k_0 distribution (Figure 6). The permeability is almost restored to its original values, i.e., the plastic effects are very weak. Thus, calculations show that an increase in γ_ε and γ_k leads to an increase in plastic effects. When these parameters tend to infinity, a completely irreversible mode of change of ε_s and k/k_0 is obtained, i.e., a purely plastic regime.

An analysis of the change in filtration characteristics during the repeated loading of the system after rest (unloading) was given based on Equation (17) with Equations (18)–(20) in a discretized form (35). The difference equations for (17) are composed in the same way as Equations (9) and (14).

Some results of numerical calculations are shown in Figures 7–9. The growth dynamics of the cake thickness both for the first and the second loading of the system are shown in Figure 7. It can be seen from the graph that the growth of the layer does not occur during unloading, and with repeated loading, a further increase in the thickness of the sediment is observed. This is a consequence of the assumption made above that the thickness of the deposit remains unchanged when the system is unloaded. Strictly speaking, the thickness of the cake after unloading, i.e., in the unloading mode, can change due to the repacking of solid particles, reduction in compressive stress between particles, and changes in porosity, compression pressure, etc. However, these factors are not considered here. In general, both in the first and second modes of loading the system, a monotonous increase in the thickness of the cake occurs.

Figure 8 shows the distribution of compression pressure p_s, solids concentration ε_s and relative permeability k/k_0 of the cake when the system is reloaded. Residual deformations after unloading affect the nature of the subsequent deformation of the sediment.

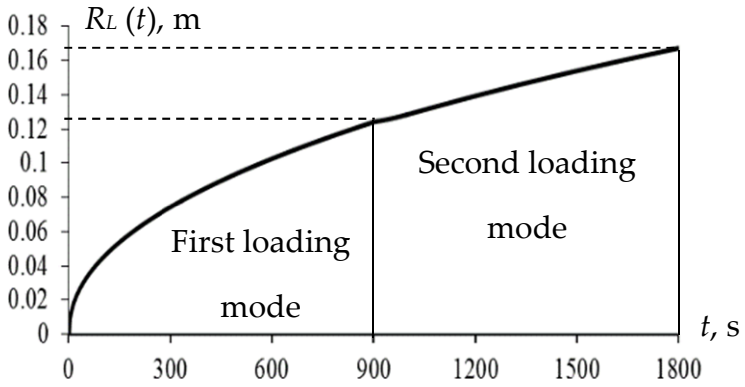

Figure 7. Dynamics of the cake thickness at $\gamma_\varepsilon = 0.6$, $\gamma_k = 0.6$.

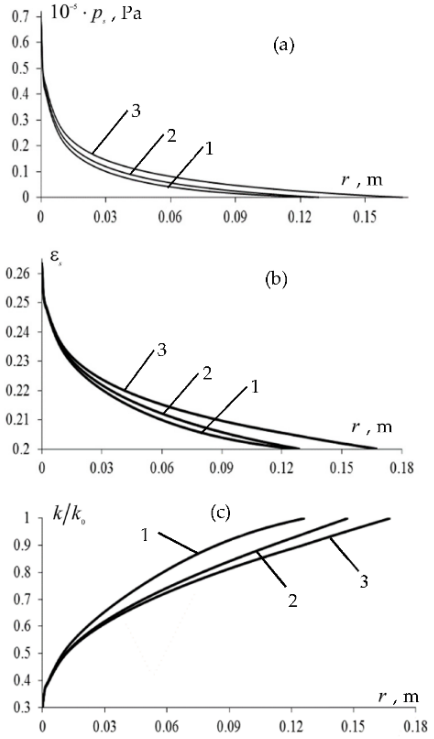

Figure 8. Distribution of p_s (**a**), ε_s (**b**), k/k_0 (**c**) in the mode of repeated loading at $\gamma_\varepsilon = 0.6$, $\gamma_k = 0.6$; 1—($t = 50$), 2—($t = 100$), 3—($t = 450$), 4—($t = 900$ s).

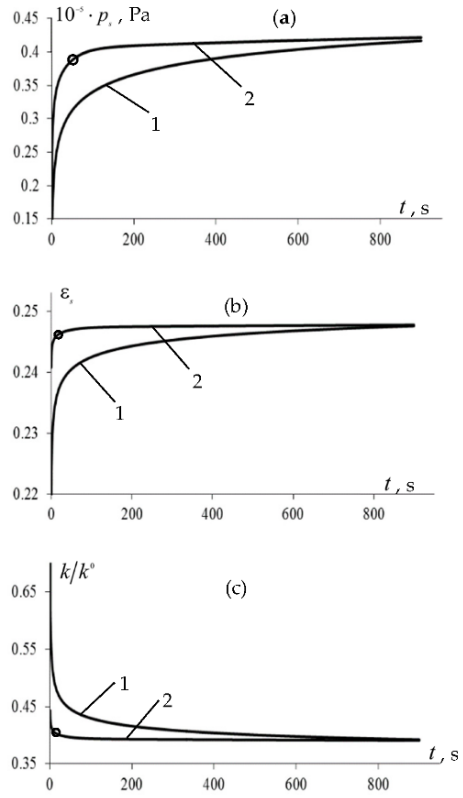

Figure 9. Dynamics of p_s (**a**), ε_s (**b**), k/k_0 (**c**) in the point $x = 0.002$ m at the first (1) and second (2) loading modes,$\gamma_\varepsilon = 0.6$, $\gamma_k = 0.6$.

There is a further change in the characteristics starting from the last state, partially restored in the unloading mode after the first loading. The model parameters characterizing

the plastic properties of cake layer deformation in the first loading mode may be different in the second loading mode.

The change in filtration characteristics at individual points of the cake layer is shown in Figure 9. As can be seen from the graphs, when the system is reloaded, there is a further increase in the compression pressure and the concentration of solid particles at a fixed point of the cake. The relative permeability decreases significantly when the system is reloaded. Primary loading and residual effects in the unloading mode significantly change the initial state of the system before the repeated (second) loading of the system, which affects the filtration characteristics in the repeated loading mode.

Figure 9 shows the dynamics of characteristics at a given point for both loadings. As can be seen from the figure, the plastic deformation of the sediment layer significantly alters the dynamics of changes in characteristics under repeated loading. At the same time, the system quickly reaches the state of the first loading, and filtering occurs according to its conditions. The circles on the graphs show the state of reaching the compressive pressure p_s to $p_s^{(1)}$ value upon reloading.

Note that only the results of Figures 3 and 4 can be explained in terms of the usual cake filtration models. The results of Figures 5 and 6 reflect the change in filtration characteristics in the pressure reduction mode and were obtained based on Equation (14), derived here from Equations (15) and (16). Figures 8 and 9 correspond to the solution of Equation (17), which was derived from Equations (18)–(20). Therefore, the results shown in Figures 5, 6, 8 and 9, and the loading mode of Figure 7, cannot be obtained and explained within the framework of the classical theory of cake filtration.

5. Conclusions

This paper considers the axisymmetric problem of filtering a suspension with the formation of an elastic–plastic cake. It is supposed that the cake is formed on the filter surface, consisting of solid suspension particles, the thickness of which monotonically increases during filtration. Filtration characteristics in the cake, such as the concentration of solid particles, the relative permeability of the layer after unloading the system, when the compression pressure and the pressure in the liquid phase are reduced to zero, are not restored to their original values. This is due to the plastic deformation of the cake layer during the first loading of the system. When the system is reloaded, i.e., during the resumption of filtration, there is a further change in filtration parameters depending on the residual state of the system after the unloading mode.

For all these regimes, suspension filtration equations were derived considering the partial irreversibility of cake deformation. Separately, an equation was derived that described the increase in the thickness of the cake during filtration. For these equations, filtering problems were numerically formulated and solved. Since the mathematical model includes an unknown moving boundary, for calculating the thickness of the cake, in the numerical solution by the finite difference method, a special technique was used called "catching the front", along the spatial coordinates at a given time step. The systems of nonlinear difference equations were solved by the iterative method. The iterative scheme was constructed in such a way that, at each iterative step, a system of linear difference equations was obtained, which were solved by the elimination method (Tomas' algorithm). Numerical results were obtained in all three modes: first loading, unloading, second loading.

In all modes, the influence of the model parameters characterizing the plastic properties of cake deformation on the filtration performance was studied. It was shown that plastic (residual) deformations of the cake significantly affected the distribution of compression pressure, particle concentration, and relative permeability of the cake. At the same time, the parameters of plasticity in terms of particle concentration (γ_ε) and permeability (γ_k) mainly affected the corresponding indicators, i.e., on the particle concentration distribution and on the relative permeability of the cake. The higher the values of these parameters, the more pronounced the plastic properties of the cake.

Within the framework of the compiled model at $\gamma_\varepsilon \to \infty$, $\gamma_k \to \infty$, a purely plastic regime was obtained. The results of numerical calculations show a monotonic increase in the thickness of the cake layer. It was shown that the filtering characteristics during repeated loading of the system were determined by the initial state that occurred after unloading the first loading mode. In this case, the plasticity parameters γ_ε and γ_k for the second loading mode may be different from those in the first mode. In general, the mathematical model proposed here gives physically reasonable and correctly interpreted results.

The results obtained can be used in the analysis of suspension purification processes by filtering them through radial filters in various cyclic loading and unloading modes.

Author Contributions: Investigation: B.K.K., U.S., G.I. and N.W. The authors contributed equally. All authors have read and agreed to the published version of the manuscript.

Funding: This research is made possible by the Fundamental Research Grant Scheme by the Ministry of Higher Education of Malaysia (Ref: FRGS/1/2019/STG06/UPM/02/11).

Institutional Review Board Statement: Not applicable.

Informed Consent Statement: Not applicable.

Data Availability Statement: Not applicable.

Acknowledgments: The authors are grateful to anonymous reviewers for useful comments, which helped us to improve the manuscript.

Conflicts of Interest: The authors declare no conflict of interest.

References

1. Tien, C.; Bai, R.; Ramarao, B.V. Analysis of cake growth in cake filtration: Effect of fine particle retention. *AIChE J.* **1997**, *43*, 33–44. Available online: http://scholarbank.nus.edu.sg/handle/10635/67365 (accessed on 28 March 2022). [CrossRef]
2. Tien, C. *Principles of Filtration*, 1st ed.; Elsevier: Amsterdam, The Netherlands, 2012. [CrossRef]
3. Tien, C.; Ramarao, B.V. *Granular Filtration of Aerosols and Hydrosols*; Elsevier Science & Technology Books: Syracuse, NY, USA, 2007; p. 522. [CrossRef]
4. Tien, C. *Introduction to Cake Filtration: Analysis, Experiments, and Applications*, 1st ed.; Elsevier: Amsterdam, The Netherlands, 2006; p. 304.
5. Zhuzhikov, V.A. *Filtration. Theory and Practice of Separation of Suspensions*; Khimia Publish: Moscow, Russia, 1980; p. 440.
6. Fedotkin, I.M.; Vorobev, E.I.; Vyun, V.I. *Hydrodynamic Theory of Suspension Filtration*; Vishashkola Publisher: Kiev, Ukraine, 1986; p. 166.
7. Fedotkin, I.M. *Mathematical Modelling of Technological Processes*; Vishashkola Publisher: Kiev, Ukraine, 1988; p. 415.
8. Mortimer, C.J.; Burke, L.; Wright, C.; Wright, C. Microbial interactions with nanostructures and their importance for the development of electrospun nanofibrous materials used in regenerative medicine and filtration. *J. Microb. Biochem. Technol.* **2016**, *8*, 195–201. [CrossRef]
9. Alinezhad, E.; Haghighi, M.; Rahmani, F.; Keshizadeh, H.; Abdi, M.; Naddafi, K. Technical and economic investigation of chemical scrubber and biofiltration in removal of H2S and NH3 from wastewater treatment plant. *J. Environ. Manag.* **2019**, *241*, 32–43. [CrossRef]
10. Li, S.; Xie, B.; Hu, S.; Jin, H.; Liu, H.; Tan, X.; Zhou, F. Removal of dust produced in the roadway of coal mine using a mining dust filtration system. *Adv. Powder Technol.* **2019**, *30*, 911–919. [CrossRef]
11. Lim, A.E.; Lim, C.Y.; Lam, Y.C. Electroosmotic flow hysteresis for dissimilar anionic solutions. *Anal. Chem.* **2016**, *88*, 8064–8073. [CrossRef] [PubMed]
12. Lim, A.E.; Lam, Y.C. Electroosmotic Flow Hysteresis for Fluids with Dissimilar pH and Ionic Species. *Micromachines* **2021**, *12*, 1031. [CrossRef] [PubMed]
13. Tosun, I. Formulation of cake filtration. *Chem. Eng. Sci.* **1986**, *41*, 2563. [CrossRef]
14. Brenner, H. Three-Dimensional Filtration on a Circular Leaf. *AIChE J.* **1961**, *7*, 666–671. [CrossRef]
15. Sacramento, R.N.; Yang, Y.; You, Z.; Waldmann, A.; Martins, A.L.; Vaz, A.S.; Zitha, P.L.; Bedrikovetsky, P. Deep bed and cake filtration of two-size particle suspension in porous media. *J. Pet. Sci. Eng.* **2015**, *126*, 201–210. [CrossRef]
16. Ruth, B.F.; Montillon, G.H.; Montonna, R.E. Studies in filtration II. Fundamental axiom of constant pressure filtration. *Ind. Eng. Chem.* **1933**, *25*, 153. [CrossRef]
17. Grace, H.P. Resistance and compressibility of filter cakes. Part I. *Chem. Eng. Prog.* **1953**, *49*, 303–318.
18. Grace, H.P. Resistance and compressibility of filter cakes. Part II: Under conditions of pressure filtration. *Chem. Eng. Prog.* **1953**, *49*, 367–377.

19. Shirato, M.; Iwata, M.; Wakita, M.; Murase, T.; Hayashi, N. Constant rate expression of semisolid materials. *J. Chem. Eng. Jpn.* **1987**, *20*, 1–6. [CrossRef]
20. Vorobiev, E. Model of the filtration process for suspensions with compressible cakes. *Theor. Fundam. Chem. Technol. Acad. Sci. USSR* **1983**, *17*, 147–153.
21. Atsumi, K.; Akiyama, T.A. Study of cake filtration. Formulation as a Stefan problem. *Chem. Technol.* **1979**, *31*, 487–492. [CrossRef]
22. Wakeman, R.J. A numerical integration of the differential equations describing the formation of and flow in compressible filter cakes. *Trans. IChemE* **1978**, *56*, 258–265.
23. Ismail, T.; Willis, M. Brief communication fluid velocity variation in filter cakes. *Int. J. Multiph. Flow* **1983**, *9*, 763–766.
24. Stamatakis, K.; Tien, C. Cake formation and growth in cake filtration. *Chem. Eng. Sci.* **1991**, *46*, 1917–1933. [CrossRef]
25. Landman, K.A.; White, L.R.; Eberl, M. Pressure filtration of flocculated suspensions. *AIChE J.* **1995**, *41*, 1687–1700. [CrossRef]
26. Tien, C.; Bai, R. An assessment of the conventional cake filtration theory. *Chem. Eng. Sci.* **2003**, *58*, 1323. [CrossRef]
27. Burger, R.; Concha, F.; Karlsen, K.H. Phenomenological model of filtration processes. Cake formation and expression. *Chem. Eng. Sci.* **2001**, *56*, 4537–4553. [CrossRef]
28. Vorobiev, E.; Tarasenko, A. Effect of cake compressibility on suspension filtration process regularities. *Theor. Fundam. Chem. Technol. Acad. Sci. USSR* **1987**, *21*, 507–513.
29. Vorobjov, E.I.; Anikeev, J.V.; Samolyotov, V.M. Dynamics of filtration and expression: New methods for combined analysis and calculation of the processes with due to account of the cake consolidation dynamics and the filter medium compressibility. *Chem. Eng. Process.* **1993**, *32*, 45–51. [CrossRef]
30. Khuzhayorov, B.K.; Saydullaev, U.Z.; Kholiyarov, E.C. Numerical solution of the suspensions filtering equations with forming an elasto–Plastic cake layer. *Uzb. J. Probl. Mech.* **2015**, *1*, 38–41.
31. Khuzhayorov, B.K.; Saydullaev, U.Z. Solution of a suspension filtration equation with forming an elasto-plastic cake layer. *Sci. J. Samarkand State Univ.* **2017**, *1*, 97–103.
32. Rezaei, A.; Abdollahi, H.; Gharabaghi, M.; Mamghaderi, H. Studies on the effects of physical parameters of filtration process on the fluid flow characteristics and de-watering efficiency of copper concentrate. *Int. J. Min. Geo-Eng. IJMGE* **2021**, *55*, 109–116.
33. Li, S.; Xing, Y.; Honglei, S.; Xiaodong, P.; Zonghao, Y.; Yuanqiang, C. A new approach for determining compressibility and permeability characteristics of dredged slurries with high water content. *Can. Geotech. J.* **2021**, *99*, 1–13. [CrossRef]
34. Khuzhayorov, B.K.; Saydullayev, U.J. Numerical solution of relaxation filtration equations with forming a consolidating cake layer. *Int. J. Adv. Res. Sci. Eng. Technol.* **2018**, *5*, 5102–5110.
35. Khuzhayorov, B.K.; Saydullaev, U.; Fayziev, B. Relaxation Equations of Consolidating Cake Filtration. *J. Adv. Res. Fluid Mech. Therm. Sci.* **2020**, *74*, 168–182. [CrossRef]
36. Barenblatt, G.I.; Krylov, A.P. On the elastic–plastic regime of flow in porous media. *Izv. Akad. Nauk SSSR OTN* **1955**, *2*, 5–13.
37. Khuzhayorov, B.K.; Davidenko, M.A.; Shodmonov, I.E. Filtration of a homogeneous liquid at the elastic–plastic regime with destruction of beds. *Uzb. J. Probl. Mech.* **1997**, *3*, 40–43.
38. Khuzhayorov, B.K.; Shodmonov, I.E.; Kholiyarov, E.C.; Zokirov, A.A. Elastoplastic Filtration of Liquid in Unstable Seams. *J. Eng. Phys. Thermophys.* **2003**, *76*, 1340–1347. [CrossRef]
39. Khuzhayorov, B.K.; Kholiyarov, E.C. Inverse problems of elastoplastic filtration of liquid in a porous medium. *J. Eng. Phys. Thermophys.* **2007**, *80*, 517–525. [CrossRef]
40. Samarsky, A.A. *Finite-Difference Schemes Theory*; Nauka: Moscow, Russia, 1977.
41. Samarskiy, A.A.; Vabishchevich, P.N. *Computational Heat Transfer*; Editorial URSS: Moscow, Russia, 2003; p. 784.